

RESUSCITATED VARIATION MODEL FOR IMAGE DEHAZING

¹Prof. M. Sessaiah, ²Farhiz Pasha, ³Ashwini R, ⁴Kavya D N

¹Assistant Professor, Dept. of CSE, S J C Institute of Technology, Chickaballapur, Karnataka, India.

²student Dept. of CSE, S J C Institute of Technology, Chickaballapur, Karnataka, India

³student Dept. of CSE, S J C Institute of Technology, Chickaballapur, Karnataka, India

⁴student Dept. of CSE, S J C Institute of Technology, Chickaballapur, Karnataka, India

ABSTRACT: Fuzzy-view photography usually suffers from low-contrast, which reduces the visibility of the scene. The performance of single-image dehazing methods is limited by the constraints or the restrictions. In this paper, we present an effective method for fog removal, which uses retrieved correlated fog-free images as external information. The proposed variable model includes two standard regularization rules to prevent visual transmission and transverse visual illumination, which are best applied in the image dehazing area. In contrast to the traditional two-stage framework, our proposed model simultaneously integrates the transmission estimation stage and image retrieval stage into a unified prediction model to obtain accurate transmission map and retrieved visual illumination. Experiments on various simulated and real-world blurred images suggest that the proposed algorithm yields better results compared to many advanced dehazing and enhancement techniques.

Introduction

Outdoor images taken during fog and fog days are characterized by low visibility and faded colors due to disturbing media in the atmosphere, which adversely affects many open computer vision applications. In addition, high-level computer vision functions such as detection, identification, tracking, classification, and so on are images or videos captured by the camera that have high visibility and clear visual features. Therefore, blur removal is an important pre-processing step for high-level vision tasks, and at the same time has great importance and value in the field of image processing and computer vision for the sea e.g. Exploration [1], [2], remote sensing [3], natural image enhancement [4] and so on. Eliminating fog is usually a challenging problem

Visual transmission is based on unfamiliar depth information that changes at different locations. Therefore, the first decoupling algorithms exploit

multiple images or additional information to retrieve the main hazy image. Dehazing techniques based on multiple images are obscured by polarized filtered images [5], [6] or two or more input images can be operated in a single scene [7], [8] under different climatic conditions. She removes. Other depth-based dehazing techniques [9], [10] use visual depth information from known three-dimensional (3D) models or user input. However, these methods are limited in real applications because additional information or multiple input images are not always available. Therefore, restoring a clear image from a recently delivered single image has attracted more attention. Some researchers aim to improve contrast and color from the image enhancement perspective, such as histogram-based [9], contrast-based [10], fusion-based [1], [ret] retinex-based [5], [5].] And so on. Unfortunately, improvement-based dehazing techniques cannot be completely overcome due to the opacity for failing to consider the image degradation mechanisms. In contrast, physics-based dehazing algorithms first construct blur imaging models, then estimate unknown parameters, and ultimately invert the physical model to obtain a blur-free image, starting from the cause of image degradation. However, these methods usually require hand-crafted priors or beliefs to solve this sickness problem. Based on this attribute, many priors or beliefs propose to estimate key parameters from a single blurred image. To reduce complexity, it is time-consuming [2], medium filters [1], guided filters [2], semi-global adaptive filters [3] and fast averaged filters [4] instead of classical median filters. 5] Adapted to improve visual transmission map. In addition, the rapid implementation of the DCP-based algorithm for video decoupling has also been investigated [6]. [Grad], Gradually residual minimization threshold [RAW], partition-based strategy [4], [10], depth-localized total variance determination [3], protected fog elimination method [2], and data-driven estimation of fog density [3] proposed to obtain an accurate broadcast map. In addition, some new priors, namely color attenuation prior [4], color-line prior [5] and haze-line prior [6], are also subsequently put forward for reliable transmission estimation.

BACKGROUND WORK

Depth map reconstruction for underwater Kinect camera using inpainting and local image mode filtering
Authors: Huimin Lu, Yin Zhang, Yujie Li, Quan Zhou, Ryunosuke Tadoh, Tomoki Uemura.

The depth map gives important information for many applications of the postprocessing. In this paper, we propose a Kinect-based underwater depth map estimation method that uses a captured coarse depth map by Kinect with the loss of depth information. To overcome the drawbacks of low accuracy of coarse depth maps, we propose a corresponding reconstruction architecture that uses the underwater dual channels prior dehazing model, weighted enhanced image mode filtering, and inpainting. Our proposed method considers the influence of mud sediments in water and performs better than the traditional methods. The experimental results demonstrated that, after inpainting, dehazing, and interpolation, our proposed method can create high-accuracy depth maps.

Disadvantage enhancement-based dehazing methods cannot fully remove the haze owing to failing to consider image degradation mechanism.

Multi-user Searchable Encryption with Fine-Grained Access Control without Key Sharing[7]
Authors: Huimin Lu, Tomoki Uemura, Dong Wang, Jihua Zhu, Zi Huang, Hyoungseop Kim

Deep-sea organism automatic tracking has rarely been studied because of a lack of training data. However, it is extremely important for underwater robots to recognize and to predict the behavior of organisms. In this paper, we first develop a method for underwater real-time recognition and tracking of multi-objects, which we call "You Only Look Once: YOLO". This method provides us with a very fast and accurate tracker. At first, we remove the haze, which is caused by the turbidity of the water from a captured image. After that, we apply YOLO to allow recognition and tracking of marine organisms, which include shrimp, squid, crab and shark. The experiments demonstrate that our developed system shows satisfactory.

Disadvantage Determine the concentration of suspended particles using intensity of light which is not successful to remove the haze of underwater images.

Haze removal for a single remote sensing image based on deformed haze imaging model[3].

The contrast of remote sensing images captured in haze condition is poor, which influences their interpretation. In

this letter, a novel dehazing algorithm based on the deformed haze imaging model is proposed. First, the model is deformed by introducing a translation term. Second, the atmospheric light and transmission are estimated according to the new model combined with dark channel prior. Lastly, the haze is successfully removed from remote sensing images using the proposed estimation algorithm.

Disadvantage The estimated transmission is insensitive to the texture of ground objects, and the dehazing effect for non uniform haze is more satisfactory than the compared method.

On principal component analysis, cosine and euclidean measures in information retrieval[9]

Introduced an automated method that only requires a single input image. This method is based on two basic observations: first, images with enhanced visibility (or clear-day images) have more contrast than images plagued by bad weather; second, airlight whose variation mainly depends on the distance of objects to the viewer, tends to be smooth. Relying on these two observations, we develop a cost function in the framework of Markov random fields, which can be efficiently optimized by various techniques, such as graph-cuts or belief propagation.

Disadvantage Proposed method is solely to maximize the contrast of the degraded image under the assumption that haze-free images possess higher contrast than hazy images. However, the results by Tan's method are prone to over-saturation.

PROPOSED UNIFIED VARIATIONAL MODEL

Recent research in [55] suggests that Retinex is considered a solution to the image problem at the inverse intensity of the input image $I(x)$. What's more, the liner relationship between image decoding and retinex is theoretically proven at both the algorithmic level and the modulation level. Mathematically, its relationship can be described as: $Dehazing(I(x)) = 1 - Retinex(1 - I(x))$ (5) Inspired by this relationship between dehazing and retinex, we solve the image problem. Retinex by distorting the atmospheric scattering pattern. To make the image dehydrating problem in Retinex solution, the traditional atmospheric scattering model (1) must be converted to Retinex by dividing the global atmospheric light A on either side of the formula (1). The traditional solution is to shift the logarithmic domain (7) to reduce the computational complexity. However, the gradient variation of bright fields is suppressed and the logarithmic transformation is not optimal for generating the term regularization in the variable model [54]. This is due to the fact that the logarithmic transformation of the

regularization terms increases errors in some limitations compared to others. In addition, using classical retinex-based algorithms directly for image dosing is inappropriate and may lead to color distortion or halo artifacts.

PROBLEM DEFINITION

The deterioration performance of the proposed unified variable model is estimated by comparing the seven most advanced methods, including density, with hand-drawn pre-based methods [19], [28], [30], [34]. Fog evaluation-based method [62] and machine learning-based methods [43], [4]. In [19], guided filters [22] are adopted to improve visual transmission to increase computational efficiency. For an unbiased comparison, the parameters of these methods are determined according to the relevant articles.

IMPLEMENTATION

In our experiments, the parameters α , β , λ_1 and λ_2 were similarly set to 0.1, 0.1, 0.1 and 10. In the next subsection, a detailed exploration of the parameters is carried out. In practice, empirical setting parameters give descending results in most cases. For input color blur images, two specific approaches are used. One method, in particular, is to convert the color image to HSV color space (color, saturation and value), and then deal with the value channel only and return the final processed result to the RGB color space. The second approach is to manage each color channel (red, green, and blue) separately. In general, processing each color channel for input color images is a conduit for improving color. Following this standard, our proposed integrated version model is encountered in this paper with each color channel for color correction. For the visual transmission of each color channel, the final visual transmission is only three channels on average due to its similarity. In addition, gamma correction ($\gamma = 0.75$) is also performed to improve visual effects and increase its brightness. When one parameter is changed, the other weighted parameters are kept as default values. Fig. 5 and Fig. 6. As can be seen from Fig. 6, the details of the recovered visual illumination are progressively blurred, and the unwanted textures of visual transmission predicted by the increase of visual and λ_1 do not go smoothly. This is because α and λ_1 control the sensitivity of the visible brightness.

Algorithm 1 Solution of Proposed Unified Model (8)

- (1) **Input:** Hazy image $I(x)$, parameters $\alpha, \beta, \lambda_1, \lambda_2$
- (2) Estimate the atmospheric light A using [19].
- (3) Estimate the initial transmission t_0 using (21) based on morphological dark channel.
- (4) **Initialization:** $T^0 = t_0, R^0 = b^0 = v^0 = 0$
- (5) **Iteration:** iterate on $k = 1, 2, \dots, K$
 - (a) Update d^k using (11);
 - (b) Update R^k using (14);
 - (c) Update b^k using (15);
 - (d) Correct R^k using $\max(R^k, 1)$;
 - (e) Update u^k using (18);
 - (f) Update T^k using (19);
 - (g) Update v^k using (20);
 - (h) Correct T^k using $\max(\min(1, T^k), 0)$;
- (6) **Output:** R^k, T^k

Parameters sensitivity experiments

Here we will investigate the influence on the estimated scene transmission and the recovered scene radiance caused by the changes of four important parameters. To measure the impact of each weighted parameters respectively, we adopt the variable-controlling approach that changes the value of one parameter while keeping other parameters unchanged. The default values of parameters α, λ_1, β , and λ_2 are set as 0.1, 0.1, 0.1, and 10 respectively.

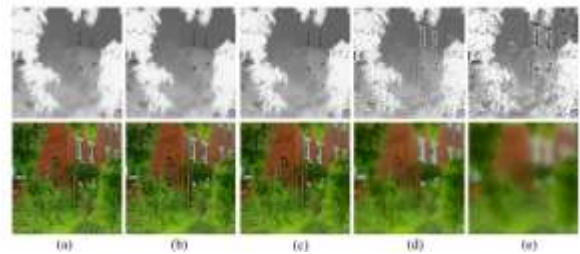


Figure 5. Impact of parameter α . First row: estimated scene transmission. Second row: recovered scene radiance. (a) $\alpha = 0.01$. (b) $\alpha = 0.1$. (c) $\alpha = 1$. (d) $\alpha = 10$. (e) $\alpha = 100$.

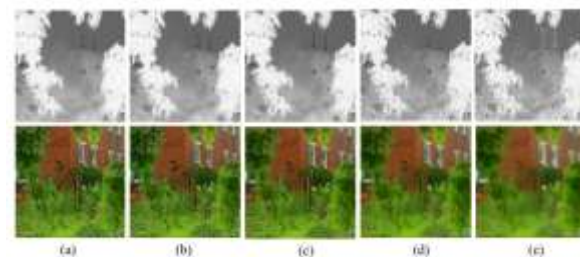


Figure 6. Impact of parameter λ_1 . First row: estimated scene transmission. Second row: recovered scene radiance. (a) $\lambda_1 = 0.01$. (b) $\lambda_1 = 0.1$. (c) $\lambda_1 = 1$. (d) $\lambda_1 = 10$. (e) $\lambda_1 = 100$.

When altering one parameter, other weighted parameters are kept the default values. As can be seen from Fig. 5 and Fig. 6, the details of the recovered scene radiance are gradually blurred and the unwanted textures of the estimated scene transmission are gradually not smoothed with the increase of α and λ_1 . This is because α and λ_1 control the smoothness of the scene radiance. In Fig. 7, as β increase, the recovered image tends to generate halo artifacts at depth discontinuities and damage the image details in the upper left corner, and meanwhile the estimated scene transmission cannot preserve the overall structures. When increasing λ_2 gradually, we find that the textures in the estimated transmission first are smoothed effectively and then the smoothness effects may be invalid once the value of λ_2 is too large. This is due to that β and λ_2 dominate the texture-smoothing and structure-preserving property of the scene transmission. According to the properties of these four regularization parameters, we optimally select the relatively appropriate value of these regularization parameters as the default values. In most cases, the default setting of parameters can produce the descent scene radiance and the structure-preserving scene transmission in a simultaneous manner.

CONCLUSION

We have introduced a simple but efficient integrated variable model for single image dehazing. Based on the relationship between image dehazing and retinex, the dehazing problem is modeled as a minimization of the variable model, which contains two total differential regularization terms to prevent transmission and transverse visual illumination, respectively. The optimization process can be solved by an alternate direction reduction scheme. In contrast to the previous two-stage dehazing framework, the proposed method integrates the transmission phase and the recovery phase into a variable equation that can simultaneously predict the visual transmission and retrieve the blurred image. Subject and objective comparisons with other state-of-the-art dehazing and enhancement techniques are conducted to ensure that our proposed method works better on improved performance or deterioration efficiency and color reliability.

Bibliography

[1] H. Lu et al., "Depth map reconstruction for underwater Kinect camera using inpainting and local image mode filtering," *IEEE Access*, vol. 5, pp. 7115–7122, 2017.
 [2] H. Lu, T. Uemura, D. Wang, J. Zhu, Z. Huang, and H. Kim, "Deep-sea organisms tracking using dehazing and deep learning," in *Mobile Networks and Applications*. Berlin, Germany: Springer, 2018, pp. 1–8.
 [3] X. Pan, F. Xie, Z. Jiang, and J. Yin, "Haze removal for a single remote sensing image based on deformed haze imaging model," *IEEE Signal*

Process. Lett., vol. 22, no. 10, pp. 1806–1810, Oct. 2015.
 [4] Y. Gong and I. F. Sbalzarini, "Image enhancement by gradient distribution specification," in *Proc. Asian Conf. Comput. Vis. (ACCV)*. Berlin, Germany: Springer, 2014, pp. 47–62.
 [5] Y. Y. Schechner, S. G. Narasimhan, and S. K. Nayar, "Instant dehazing of images using polarization," in *Proc. IEEE Conf. Comput. Vis. Pattern Recognit. (CVPR)*, Dec. 2001, p. 1.
 [6] S. Shwartz, E. Namer, and Y. Y. Schechner, "Blind haze separation," in *Proc. IEEE Comput. Soc. Conf. Comput. Vis. Pattern Recognit. (CVPR)*, vol. 2, Jun. 2006, pp. 1984–1991.
 [7] S. G. Narasimhan and S. K. Nayar, "Chromatic framework for vision in bad weather," in *Proc. IEEE Conf. Comput. Vis. Pattern Recognit. (CVPR)*, vol. 1, Jun. 2000, pp. 598–605.
 [8] S. G. Narasimhan and S. K. Nayar, "Contrast restoration of weather degraded images," *IEEE Trans. Pattern Anal. Mach. Learn.*, vol. 25, no. 6, pp. 713–724, Jun. 2003.
 [9] J. Kopf et al., "Deep photo: Model-based photograph enhancement and viewing," *ACM Trans. Graph.*, vol. 27, no. 5, pp. 116:1–116:10, Dec. 2008.
 [10] S. G. Narasimhan and S. K. Nayar, "Interactive deweathering of an image using physical models," in *Proc. IEEE Workshop Color Photometric Methods Comput. Vis.*, Nice, France, Oct. 2003, vol. 6, no. 6.4, pp. 1–7.
 [11] Z. Xu, X. Liu, and X. Chen, "Fog removal from video sequences using contrast limited adaptive histogram equalization," in *Proc. Int. Conf. Comput. Intell. Softw. Eng. (CISE)*, Dec. 2009, pp. 1–4.
 [12] Z. Mi, H. Zhou, Y. Zheng, and M. Wang, "Single image dehazing via multi-scale gradient domain contrast enhancement," *IET Image Process.*, vol. 10, no. 3, pp. 206–214, 2016.
 [13] C. O. Ancuti and C. Ancuti, "Single image dehazing by multi-scale fusion," *IEEE Trans. Image Process.*, vol. 22, no. 8, pp. 3271–3282, Aug. 2013.
 [14] Y. Li, Q. Miao, R. Liu, J. Song, Y. Quan, and Y. Huang, "A multi-scale fusion scheme based on haze-relevant features for single image dehazing," *Neurocomputing*, vol. 283, pp. 73–86, Mar. 2018.
 [15] J. Zhou and F. Zhou, "Single image dehazing motivated by retinex theory," in *Proc. 2nd Int. Symp. Instrum. Meas., Sensor Netw. Automat. (IMSNA)*, Dec. 2013, pp. 243–247.
 [16] J. Wang, K. Lu, J. Xue, N. He, and L. Shao, "Single image dehazing based on the physical model and MSRCR algorithm," *IEEE Trans. Circuits Syst. Video Technol.*, vol. 28, no. 9, pp. 2190–2199, Sep. 2018.
 [17] R. T. Tan, "Visibility in bad weather from a single image," in *Proc. IEEE Conf. Comput. Vis. Pattern Recognit. (CVPR)*, Anchorage, AK, USA, Jun. 2008, pp. 1–8.
 [18] R. Fattal, "Single image dehazing," *ACM Trans. Graph.*, vol. 27, no. 3, p. 72, Aug. 2008.
 [19] K. He, J. Sun, and X. Tang, "Single image haze removal using dark channel prior," *IEEE Trans. Pattern Anal. Mach. Intell.*, vol. 33, no. 12, pp. 2341–2353, Dec. 2011.
 [20] K. B. Gibson, D. T. Vo, and T. Q. Nguyen, "An investigation of dehazing effects on image and video coding," *IEEE Trans. Image Process.*, vol. 21, no. 2, pp. 662–673, Feb. 2012.
 [21] J.-P. Tarel and N. Hautière, "Fast visibility restoration from a single color or gray level image," in *Proc. IEEE 12th Conf. Comput. Vis. Pattern Recognit. (CVPR)*, Sep./Oct. 2009, pp. 2201–2208.
 [22] K. He, J. Sun, and X. Tang, "Guided image filtering," *IEEE Trans. Pattern Anal. Mach. Intell.*, vol. 35, no. 6, pp. 1397–1409, Jun. 2013.
 [23] H. Lu, Y. Li, S. Nakashima, and S. Serikawa, "Single image dehazing through improved atmospheric light estimation," *Multimedia Tools Appl.*, vol. 75, no. 24, pp. 17081–17096, 2016.
 [24] W. Wang, F. Chang, T. Ji, and X. Wu, "A fast single-image dehazing method based on a physical model and gray projection," *IEEE Access*, vol. 6, pp. 5641–5653, 2018.
 [25] A. Levin, D. Lischinski, and Y. Weiss, "A closed-form solution to natural

image matting," *IEEE Trans. Pattern Anal. Mach. Intell.*, vol. 30, no. 2, pp. 228–242, Feb. 2008.

[26] Y. Park and T.-H. Kim, "Fast execution schemes for dark-channel-priorbased outdoor video dehazing," *IEEE Access*, vol. 6, pp. 10003–10014, 2018.

[27] G. Meng, Y. Wang, J. Duan, S. Xiang, and C. Pan, "Efficient image dehazing with boundary constraint and contextual regularization," in *Proc. IEEE Int. Conf. Comput. Vis.*, Dec. 2013, pp. 617–624.

[28] C. Chen, M. N. Do, and J. Wang, "Robust image and video dehazing with visual artifact suppression via gradient residual minimization," in *Proc. ECCV*, 2016, pp. 576–591.

[29] H. Yuan, C. Liu, Z. Guo, and Z. Sun, "A region-wised medium transmission based image dehazing method," *IEEE Access*, vol. 5, pp. 1735–1742, 2017.

[30] Y. Liu, H. Li, and M. Wang, "Single image dehazing via large sky region segmentation and multiscale opening dark channel model," *IEEE Access*, vol. 5, pp. 8890–8903, 2017.

[31] Q. Liu, X. Gao, L. He, and W. Lu, "Single image dehazing with depth-aware non-local total variation regularization," *IEEE Trans. Image Process.*, vol. 27, no. 10, pp. 5178–5191, Oct. 2018.

[32] T. Zhang, H. Hu, and B. Li, "A naturalness preserved fast dehazing algorithm using HSV color space," *IEEE Access*, vol. 6, pp. 10644–10649, 2018.

[33] S. Huang, D. Wu, Y. Yang, and H. Zhu, "Image dehazing based on robust sparse representation," *IEEE Access*, vol. 6, pp. 53907–53917, 2018.

[34] Q. Zhu, J. Mai, and L. Shao, "A fast single image haze removal algorithm using color attenuation prior," *IEEE Trans. Image Process.*, vol. 24, no. 11, pp. 3522–3533, Nov. 2015.

[35] R. Fattal, "Dehazing using color-lines," *ACM Trans. Graph.*, vol. 34, no. 1, pp. 13:1–13:14, Dec. 2014.

[36] D. Berman, T. Treibitz, and S. Avidan, "Non-local image dehazing," in *Proc. IEEE Conf. Comput. Vis. Pattern Recognit. (CVPR)*, Jun. 2016, pp. 1674–1682.

[37] R. He, Z. Wang, Y. Fan, and D. D. Feng, "Multiple scattering model based single image dehazing," in *Proc. IEEE 8th Conf. Ind. Electron. Appl. (ICIEA)*, Jun. 2013, pp. 733–737.

[38] M. Ju, Z. Gu, and D. Zhang, "Single image haze removal based on the improved atmospheric scattering model," *Neurocomputing*, vol. 260, pp. 180–191, Oct. 2017.

[39] M. Ju, C. Ding, D. Zhang, and Y. J. Guo, "BDPK: Bayesian dehazing using prior knowledge," *IEEE Trans. Circuits Syst. Video Technol.*, to be published, doi: 10.1109/TCSVT.2018.2869594.

[40] M.-Y. Ju, C. Ding, D.-Y. Zhang, and Y. J. Guo, "Gamma-correction-based visibility restoration for single hazy images," *IEEE Signal Process. Lett.*, vol. 25, no. 7, pp. 1084–1088, Jul. 2018.

[41] K. Tang, J. Yang, and J. Wang, "Investigating haze-relevant features in a learning framework for image dehazing," in *Proc. IEEE Conf. Comput. Vis. Pattern Recognit. (CVPR)*, Jun. 2014, pp. 2995–3002.

[42] M. Kim, S. Yu, S. Park, S. Lee, and J. Paik, "Image dehazing and enhancement using principal component analysis and modified haze features," *Appl. Sci.*, vol. 8, no. 8, p. 1321, 2018.

[43] B. Cai, X. Xu, K. Jia, C. Qing, and D. Tao, "DehazeNet: An end-to-end system for single image haze removal," *IEEE Trans. Image Process.*, vol. 25, no. 11, pp. 5187–5198, Nov. 2016.

[44] W. Ren, S. Liu, H. Zhang, J. Pan, X. Cao, and M.-H. Yang, "Single image dehazing via multi-scale convolutional neural networks," in *Proc. ECCV*, 2016, pp. 154–169.

[45] B. Li, X. Peng, Z. Wang, J. Xu, and D. Feng, "AOD-Net: All-in-one dehazing network," in *Proc. IEEE Int. Conf. Comput. Vis. (ICCV)*, Oct. 2017, pp. 4780–4788.

[46] C. Li, J. Guo, F. Porikli, H. Fu, and Y. Pang, "A cascaded convolutional neural network for single image dehazing," *IEEE Access*, vol. 6, pp. 24877–24887, 2018.

[47] J. Li, G. Li, and H. Fan, "Image dehazing using residual-based deep CNN," *IEEE Access*, vol. 6, pp. 26831–26842, 2018.

[48] H. Koschmieder, "Theorie der horizontalen sichtweite," in *Proc. Beitrage Physik Freien Atmosphere*, 1924, pp. 33–53.

[49] E. H. Land and J. J. McCann, "Lightness and Retinex theory," *J. Opt. Soc. Amer.*, vol. 61, no. 1, pp. 1–11, 1971.

[50] E. H. Land, "The retinex theory of color vision," *Sci. Amer.*, vol. 237, no. 6, pp. 108–129, 1977.

[51] D. J. Jobson, Z.-U. Rahman, and G. A. Woodell, "Properties and performance of a center/surround Retinex," *IEEE Trans. Image Process.*, vol. 6, no. 3, pp. 451–462, Mar. 1997.

[52] D. J. Jobson, Z.-U. Rahman, and G. A. Woodell, "A multiscale Retinex for bridging the gap between color images and the human observation of scenes," *IEEE Trans. Image Process.*, vol. 6, no. 7, pp. 965–976, Jul. 1997.

[53] N. Banić and S. Lončarić, "Light random sprays retinex: Exploiting the noisy illumination estimation," *IEEE Signal Process. Lett.*, vol. 20, no. 12, pp. 1240–1243, Dec. 2013.

[54] X. Fu, D. Zeng, Y. Huang, X.-P. Zhang, and X. Ding, "A weighted variational model for simultaneous reflectance and illumination estimation," in *Proc. IEEE Conf. Comput. Vis. Pattern Recognit. (CVPR)*, Jun. 2016, pp. 2782–2790.

[55] A. Galdran, A. Alvarez-Gila, A. Bria, J. Vazquez-Corral, and M. Bertalmio, "On the duality between retinex and image dehazing," in *Proc. IEEE CVPR*, Salt Lake City, FL, USA, Jun. 2018, pp. 8212–8221.

[56] L. I. Rudin, S. Osher, and E. Fatemi, "Nonlinear total variation based noise removal algorithms," *Phys. D, Nonlinear Phenomena*, vol. 60, nos. 1–4, pp. 259–268, 1992.

AUTHORS



Ashwini R, she is undergraduate student currently pursuing B.E CS&E in SJCIT, VTU Belgaum .His current research interests include digital image processing, microprocessor.



Kavya D N, she is undergraduate student currently pursuing B.E CS&E in SJCIT, VTU Belgaum .His current research interests include digital image processing, computer graphics.



Farhiz Pasha, he is undergraduate student currently pursuing B.E CS&E in SJCIT, VTU Belgaum .His current research interests include digital image processing, machine learning.



Prof. M. Seshaiiah, Asst. professor at SJCIT, Received M.Tech. Degree in CSE from VTU, Belgaum where he is currently pursuing the Ph.D. His current research interests include digital image processing, compiler design and microprocessor & micro controllers.